

# RSC Advances



This is an *Accepted Manuscript*, which has been through the Royal Society of Chemistry peer review process and has been accepted for publication.

*Accepted Manuscripts* are published online shortly after acceptance, before technical editing, formatting and proof reading. Using this free service, authors can make their results available to the community, in citable form, before we publish the edited article. This *Accepted Manuscript* will be replaced by the edited, formatted and paginated article as soon as this is available.

You can find more information about *Accepted Manuscripts* in the [Information for Authors](#).

Please note that technical editing may introduce minor changes to the text and/or graphics, which may alter content. The journal's standard [Terms & Conditions](#) and the [Ethical guidelines](#) still apply. In no event shall the Royal Society of Chemistry be held responsible for any errors or omissions in this *Accepted Manuscript* or any consequences arising from the use of any information it contains.



Journal Name

COMMUNICATION

## Colorimetric and ultrasensitive immunosensor for one-step pathogen detection via the combination of nanoparticles-triggered signal amplification and magnetic separation

Received 00th January 20xx,  
Accepted 00th January 20xx

DOI: 10.1039/x0xx00000x

Yiping Chen<sup>a</sup> and Mengxia Xie<sup>b\*</sup>

www.rsc.org/

**We develop a visual immunosensor for the one-step detection of *Salmonella enterica* by using gold nanoparticles triggered enzyme signal amplification and magnetic separation. This immunosensor shows an enhanced sensitivity compared with enzyme-linked immunosorbent assay, without the involvement of any equipment, thus providing a promising platform for rapid and sensitive detection of pathogen.**

*Salmonella enterica* (*S. enterica*) is a common and harmful pathogen that causes food poisoning worldwide.<sup>1</sup> A relatively small number of *S. enterica* can cause severe illness such as gastroenteritis.<sup>2</sup> The outbreak of *S. enterica* has emerged as a prominent cause of death in African children.<sup>3</sup> Even for the United States, the infection by *S. enterica* leads to 370 people died per year.<sup>4</sup> *S. enterica* infection is usually transmitted to people by food chain, so that the development of an effective method for detecting *S. enterica* in food samples is highly important to prevent the outbreak of diseases. Many methods have been used to detect *S. enterica* including polymerase chain reaction (PCR),<sup>5,6</sup> enzyme-linked immunosorbent assay (ELISA),<sup>7,8</sup> gold lateral flow test (GLFT)<sup>9,10</sup> and novel biosensors such as surface plasmon resonance (SPR) sensor<sup>11,12</sup>, fluorescence method<sup>13,14</sup> and magnetic relaxation switch (MRS) sensor.<sup>15</sup> PCR is the gold standard for detection of pathogens due to its high sensitivity and selectivity, but it requires expensive instruments, laboratory of high biosafety level, and professional operators which dramatically limit its application in the resource-poor areas. ELISA has been widely used to detect pathogens because of its specificity, sensitivity, and low cost. However, ELISA is usually labor-intensive and time-consuming because of the multiple steps of operations. GLFT is also extensively used in pathogen detection due to its simplicity, rapidity, and low cost. A major limitation of GLFT is the low

sensitivity that is inferior to that of ELISA, so that GLFT may not allow for highly sensitive detection of *S. enterica*. SPR is a label-free biosensor for detecting pathogens, but its application is hindered by its poor sensitivity and high cost. In previous work, we have developed an MRS sensor for rapid and sensitive detection of *S. enterica* in one step. However, this method still relies on an instrument for signal readout, and is not suitable for point-of-care testing (POCT) or on-site detection of pathogens. To address the aforementioned issues, the development of a simple, rapid and sensitive method to detect *S. enterica* in food samples is highly necessary.

Visual readout of biochemical assays has drawn increasing attentions because it is convenient, low-cost, rapid and instrument-free.<sup>16,17</sup> At present, visual detection methods mainly include: 1) color change originated from the chemical reactions;<sup>18</sup> 2) color change based on the unique characteristics of nanoparticles,<sup>19-21</sup> such as the gold nanoparticles (AuNPs). The change of state of AuNPs in solution results in the color change, which has been widely adopted for visual readout in biochemical assays. This strategy shows high sensitivity and good stability, but it needs relatively complex surface chemistry to modify the AuNPs and therefore limits its application in real bio-analysis; 3) color change originated from the reaction between enzyme and substrate.<sup>22</sup> For example, horse radish peroxidase (HRP) can highly catalyze its substance-tetramethylbenzidine (TMB), and the color of TMB solution changes from colorless to blue dependent on the concentration of HRP. The visual signal using substrate-enzyme system may be the most effective strategy because HRP is widely used in immunoassays as a labelling enzyme with properties of good stability, high catalytic efficiency and low cost. However, HRP is usually conjugated to the secondary antibody in the commercialized products, and the labelling efficiency is too low to achieve a high sensitivity for biochemical analysis. Therefore, it is important to construct a highly efficient bio-conjugation method to label lots of HRP molecules onto one antibody molecule.

Functional nanoparticles such as gold nanoparticles (AuNPs) and magnetic beads (MBs) have recently advanced the bio-

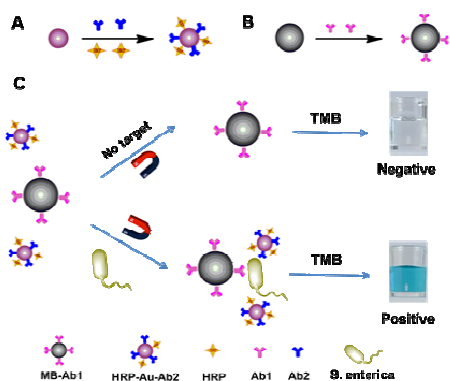
<sup>a</sup> CAS Key Lab for Biological Effects of Nanomaterials and Nanosafety, National Center for NanoScience and Technology, Beijing 100190, China.

<sup>b</sup> Analytical & Testing Center of Beijing Normal University, Beijing 100875, China  
E-mail: xiemx@bnu.edu.cn

Electronic Supplementary Information (ESI) available: [details of any supplementary information available should be included here]. See DOI: 10.1039/x0xx00000x

analysis field because of their excellent optical, magnetic or electrical properties.<sup>23-25</sup> Au NPs have been widely used in chemical and biological assays, due to their facile synthesis, high chemical stability, large specific surface area, and biocompatibility.<sup>26, 27</sup> Au NPs have a large specific surface area, and they can conjugate lots of signal molecules such as HRP. We thus hypothesize that Au NPs may be used as a carrier to simultaneously conjugate antibody (Ab) and HRP molecules to prepare the HRP-Au-Ab conjugate. HRP-Au-Ab conjugate may provide a new signal amplification system and solve the problem of low efficiency of bio-conjugation between HRP and Ab. Meanwhile, immunomagnetic separation (IMS) based on magnetic beads (MBs) can specifically capture and enrich target from complex samples. The combination of IMS with HRP-Au-Ab conjugate may specifically capture targets from complex samples, while realize signal amplification for visual readout at the same time.

In this study, we developed a simple, rapid and visual immunosensor for determination of *S. enterica* based on Au NPs-triggered enzyme signal amplification and IMS. In this immunosensor, anti-*S. enterica* antibody (Ab2) and HRP are simultaneously labeled on the surface of Au NPs to prepare the HRP-Au-Ab2 conjugate. Immunomagnetic beads (MBs-Ab1), *S. enterica* and HRP-Au-Ab2 conjugate can form a “sandwich” immunocomplex (“MB-Ab1-target-Ab2-Au-HRP”) by specific recognition between antigen and antibody. By taking the advantage of magnetic separation, this sandwich complex was separated from the complex matrix, which can highly catalyze the TMB, yielding a color change from colorless to blue that can be read with the naked eye. The brightness of the blue color is directly proportional to the concentration of *S. enterica*, and used as the visual signal. In this strategy, HRP-Au-Ab2 conjugate not only can be used as the recognition element but also as the signal amplification system since HRP can highly catalyze its substance (TMB) and the color of TMB will change from colorless to blue (Scheme 1). We use the color change of TMB solution as the readout, and the absorbance of TMB solution ( $OD_{620}$ ) for quantitative detection in this study.



**Scheme. 1** The scheme of visual immunosensor for one-step detection of *S. enterica* in milk samples. In (a), the Ab2 and HRP are simultaneously conjugated on the surface of AuNPs to

prepare the HRP-Au-Ab2 conjugate; In (b), Ab1 is labelled on the surface of MBs to form the MB-Ab1 conjugate; In (c), HRP-Au-Ab2 conjugate is used as the dual-signal probe and the signal amplification system in the immunosensor, and MB-Ab1 is used as a carrier of immunomagnetic separation to realize one-step detection of *S. enterica*.

We first characterized the property of the MBs-Ab and HRP-Au-Ab conjugate. We quantify that one magnetic beads can conjugate 52000 Ab molecules by using the bicinchoninic acid (BCA) assay kit. Very small amounts of the *S. enterica* can thus be enriched because of the high density of Ab on MB. We also characterized the Ab-Au-HRP conjugate using the biological electron microscope. Some gray floccule is labeled on the surface of Au NPs, and this gray floccule should be anti-*S. enterica* antibody and lots of HRP molecules, indicating that the Ab-Au-HRP conjugate has been successfully prepared (Figure S1).

In this immunosensor, immunomagnetic beads (MBs-Ab1) is used as the carrier to enrich *S. enterica* from samples, and HRP-Au-Ab2 conjugate is employed for signal recognition and signal amplification. We investigated three key factors that influence the sensitivity of this immunosensor: (1) The molar ratios of HRP/Ab2 on the surface of AuNPs; (2) The concentration of the MBs-Ab1 and HRP-Au-Ab2 conjugate. (3) The immune-reaction time. We chose four molar ratios of HRP/Ab (1:10, 1:50, 1:100 and 1:200) to prepare the HRP-Au-Ab2 conjugate. The  $OD_{620}$  value is the largest when the molar ratios of HRP/Ab are 100:1 and 200:1, indicating that more HRP molecules have bound on the surface of Au NPs at these molar ratios (Figure S2). The signal intensity is dependent on the amount of HRP molecules, and thus we selected the 100:1 as the ideal molar ratio of HRP/Ab for the following experiments.

When the concentration of MBs-Ab1 is too low (0.01mg/mL), it is not enough to capture the *S. enterica* in samples and the positive signal is not strong, thus affecting the accuracy of the method (Figure S3c). If the concentration of MBs-Ab1 is too high (0.1 mg/mL), the non-specific adsorption between the MBs-Ab1 and sample is severe, resulting in the false positive result (Figure S3a). High signal/noise ratio could be obtained when the concentration of MBs-Ab1 is 0.05 mg/mL (Figure S3b). Hence, 0.05 mg/mL of MBs-Ab1 was used for the following studies. These results also prove that HRP-Au-Ab2 conjugate and MBs-Ab1 have been successfully prepared. We further selected four different diluted ratios (20:1, 50:1, 100:1 and 200:1) to optimize the concentration of the HRP-Au-Ab2 conjugate. When the diluted ratio of HRP-Au-Ab2 conjugate is 1:20, we found that the color of solution in blank sample is also blue, which suggests that the non-specific adsorption between HRP-Au-Ab2 conjugate and MBs-Ab1 exists which yields a false positive result (Figure S4a). When the diluted ratio of HRP-Au-Ab2 conjugate is 1:200 and 1:500, the positive signal (the concentration of *S. enterica* is  $10^6$  cfu/mL) is not obvious (Figure S4c and Figure S4d), and the color change is not remarkable with the change of the concentration of *S. enterica*. The reason is that there is not enough HRP-Au-Ab2 conjugate to form “MBs-Ab1-target-

Ab2-Au-HRP" sandwich immune-complex. When the diluted ratio of HRP-Au-Ab2 conjugate is 1:100 (Figure S4b), the relationship between change of blue color of sample and the concentration of *S. enterica* is the most obvious, and the signal to noise ratio (S/N) is the largest, which is beneficial to the sensitivity. Thus, we adopt this diluted ratio for the following experiments.

We also optimized the reaction time from 30min, 45min and 60 min. The lowest detectable concentration of *S. enterica* is  $10^4$  cfu/mL when the reaction time is 30 min, and it can reach  $10^3$  cfu/mL when the reaction time is 45 min and 60 min (Figure S5). These results show that the whole reaction is complete when the reaction time is 45 min, which is selected as the optimized reaction time.

Under the optimized conditions, we studied the sensitivity of this method for detection of *S. enterica*. The brightness of blue color of sample increased when the concentration of *S. enterica* is from 0 cfu/mL to  $10^8$  cfu/mL (Figure 1a). We can identify the color difference between the  $10^2$  cfu/mL *S. enterica* and the blank control, and the lowest detectable concentration of the immunosensor for detection of *S. enterica* with the naked eye is  $10^2$  cfu/mL. The OD<sub>620</sub> value of samples increases when the concentration of *S. enterica* is from  $10^2$  cfu/mL to  $10^8$  cfu/mL (Figure 1b). For quantitative determination, a linear relationship between the OD<sub>620</sub> value and the log of concentration of *S. enterica* was observed in the range between  $10^3$  and  $10^7$  cfu/mL, with the linear equation  $Y = 0.127X - 0.055$  ( $X = \lg[C_{S. enterica}]$ ,  $R^2 = 0.968$ ) (Figure 1c). To investigate the performance of this visual immunosensor, we first employ GLFT as a contrast method because GLFT is a popular and simple method for naked-eye detection. The lowest detectable concentration of the GLFT for detection of *S. enterica* with the naked eye is  $10^4$  cfu/mL (Figure 1d), which suggests that the sensitivity of the visual immunosensor is superior to that of GLFT.

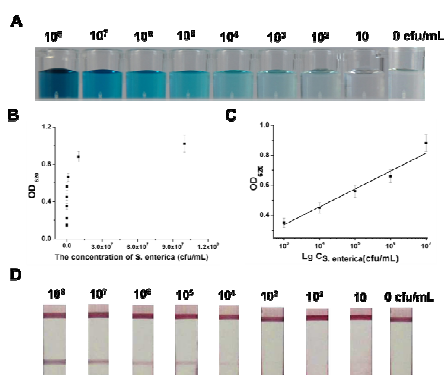


**Figure 1.** The results of visual immunosensor and GLFT for detection of *S. enterica*. (a) The visual result of this immunosensor. (b) The relationship between OD<sub>620</sub> value and the concentration of *S. enterica*. (c) The linear relationship between the OD<sub>620</sub> value and the log of concentration of *S. enterica*. (d) The result of GLFT for analysis of *S. enterica*.

ELISA was also chosen as a control method because it is widely used in detection of pathogens due to its high sensitivity and simplicity. The value of OD<sub>450</sub> increased with the concentration of *S. enterica* from 0 cfu/mL to  $10^8$  cfu/mL

(Figure S6), and the limit of detection (LOD, three times the standard deviation) is 500 cfu/mL. These results show that the sensitivity of this visual immunosensor is better than that of GLFT and ELISA. The reasons are as follows: 1) Au NPs have high specific surface areas and can conjugate lots of HRP molecules, which can be employed as the signal amplification system. In ELISA method, the signal tag is commercialized HRP-secondary conjugate, and one Ab2 molecule only conjugate one or two HRP molecules which has no obvious signal amplification effect. 2) This visual immunosensor employs magnetic separation that can enrich the target from complicated samples, giving rise to the improved sensitivity. 3) This immunosensor is a homogeneous immunoassay, and the specific recognition between antigen and antibody is more efficient, thus beneficial to the sensitivity of the analysis.

We further investigated the selectivity of the visual immunosensor. During the analysis of *S. enterica*, the other four bacteria, *Escherichia coli*, *Shigella* spp, *Staphylococcus aureus*, and *Spirillum of Cholera*, are used to evaluate the specificity of the immunosensor. The brightness of blue color of sample is remarkable in *S. enterica* group and the other bacteria samples show negligible blue color (Figure 2a), which confirms that the sensor has good specificity for detection of *S. enterica* in complex real samples. The value of OD<sub>620</sub> in *S. enterica* group is greatly larger than that of other four groups (Figure 2b), which proves that this visual immunosensor has good selectivity for detection of *S. enterica*.

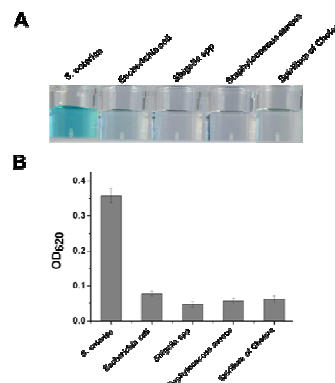


**Figure 2.** The selectivity of visual immunosensor for detection of *S. enterica*. The concentration of these bacteria was  $10^5$  cfu/mL.

Milk is often contaminated by *S. enterica*, and we detect the *S. enterica* in milk to demonstrate the practical application of this sensor. For comparison, we simultaneously employed this visual immunosensor and ELISA for the detection. The results of visual immunosensor showed that sample 1, sample 3, sample 4 and sample 5 were detected to be positive samples, and sample 2, sample 6, sample 7 and sample 8 were detected to be negative sample (Figure 3a). These results agree well with the quantitative results by using the value of OD<sub>620</sub> (Figure 3b), which further prove the accuracy of the naked eye readout strategy. The result from ELISA suggested that sample 1, sample 3 and sample 5 were detected to be positive samples and sample 2, sample 4, sample 6, sample 7 and sample 8 were detected to be negative samples (Figure 3c). Sample 1 to sample 5 were detected to be positive samples and sample 6 to

sample 8 were detected to be negative samples by PCR method in Chinese Academy of Inspection and Quarantine (Beijing, China). Real time-PCR (RT-PCR) is the gold standard for pathogen detection because of its ultrahigh sensitivity, which can reach 1cfu/mL for detection of pathogen. However, RT-PCR needs long detection time (2-3 h) and high cost, which prevent it in the field of POCT. This result showed that the accuracy rate of visual immunosensor (87%) is higher than that of ELISA (75%) because the visual immunosensor has a higher sensitivity. Compared to PCR, the advantages of this visual immunosensor are: (1) It enables naked-eye detection and needs no expensive equipment, which is very important to the on-site test; (2) It is a homogeneous immunoassay and the whole analysis can be completed in one step, which can greatly shorten the detection time.

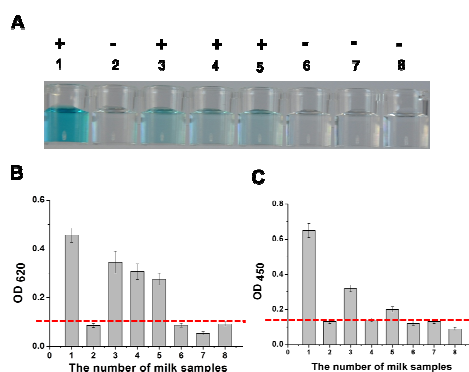


**Figure 3.** The detection of *S. enterica* in milk samples. (a) The visual result of immunosensor. (b) The quantitative result of immunosensor using absorbance of TMB solution. (c) The detection results of the ELISA. “+” present the positive sample (three times the standard deviation in blank group), “-” present the negative sample. These samples were identified to be positive sample by RT-PCR, and the concentration of these samples from 1 to 8 was  $1.5 \times 10^4$ ,  $14$ ,  $3.3 \times 10^3$ ,  $2.9 \times 10^3$ ,  $3.1 \times 10^3$ ,  $12$ ,  $14$  and  $16$  cfu/mL.

Therefore, we can apply the visual immunosensor to detect *S. enterica* in real milk samples. Compared to conventional ELISA and GLFT, this sensor has many advantages: (1) speediness and simplicity: the sensor combines the magnetic separation and visual signal generation and amplification into one step, which avoid multi-step reactions that is required in ELISA, and thus can reduce the whole analysis time (1 h). It only needs a magnetic separation rack, and does not need professional operators, which is more rapid and friendly operable than that of ELISA; (2) sensitivity: the sensitivity of this sensor for determination of *S. enterica* increases by two orders of magnitude compared with GLFT and five folds compares to that of ELISA. The visual immunosensor can be completed in short time (1 h) with convenient operation and high sensitivity, which provides an attractive method for the detection of pathogen. **Table S1** summarizes the advantages and disadvantages of ELISA, GLFT and this visual immunosensor.

## Conclusions

In summary, we have developed a simple, fast, and sensitive immunosensor for detection of *S. enterica* in milk samples by naked eyes. The enzymatic reaction between HRP and TMB is an effective visual signal readout system. Meanwhile, Au NPs is an idea carrier for signal recognition and amplification. The visual immunosensor based on magnetic separation and Au NPs-triggered enzyme signal amplification will provide a rapid, sensitive and simple platform for POCT in the fields of food safety, environment monitoring, clinical diagnosis and so on, particularly in the developing countries.

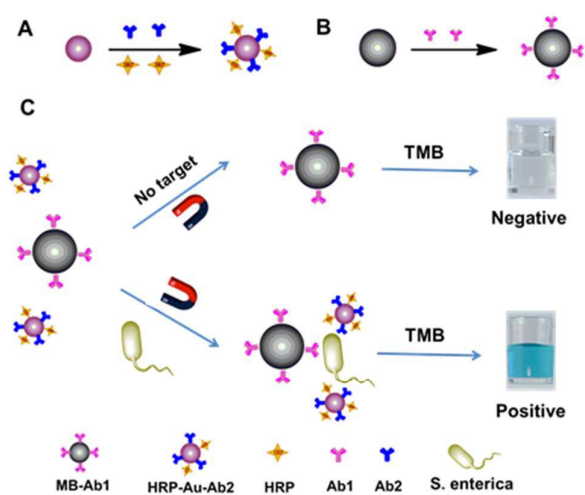
## Acknowledgement

We thank the National Science Foundation of China (21505027) for financial support.

## Notes and references

- E. Cavallaro, K. Date, C. Medus, S. Meyer, B. Miller, C. Kim, S. Nowicki, S. Cosgrove, D. Sweat, Q. Phan, J. Flint, E. R. Daly, J. Adams, E. Hyttia-Trees, P. Gerner-Smidt, R. M. Hoekstra, C. Schwensohn, A. Langer, S. V. Sodha, M. C. Rogers, F. J. Angulo, R. V. Tauxe, I. T. Williams, C. B. Behraves and S. T. Outbreak, *New. Engl. J. Med.*, 2011, **365**, 601-610.
- B. Matyas, A. Cronquist, M. Cartter, M. Tobin-D'Angelo, D. Blythe, K. Smith, S. Lathrop, D. Morse, P. Cieslak, J. Dunn, K. G. Holt, O. L. Henao, K. E. Fullerton, B. E. Mahon, R. M. Hoekstra, P. M. Griffin, R. V. Tauxe and A. Bhattarai, *Jama-J. Am. Med. Assoc.*, 2010, **303**, 2130-2132.
- N. A. Feasey, G. Dougan, R. A. Kingsley, R. S. Heyderman and M. A. Gordon, *Lancet.*, 2012, **379**, 2489-2499.
- E. Scallan, R. M. Hoekstra, F. J. Angulo, R. V. Tauxe, M. A. Widdowson, S. L. Roy, J. L. Jones and P. M. Griffin, *Emerg. Infect. Dis.*, 2011, **17**, 7-15.
- G. P. Wu, S. H. Chen and R. E. Levin, *J. Microbiol. Meth.*, 2015, **117**, 41-48.
- V. Wuyts, W. Mattheus, N. H. C. Roosens, K. Marchal, S. Bertrand and S. C. J. De Keersmaecker, *Appl. Microbiol. Biot.*, 2015, **99**, 8137-8149.
- E. Galikowska, D. Kunikowska, E. Tokarska-Pietrzak, H. Dziadziuszko, J. M. Los, P. Golec, G. Wegryzn and M. Los, *Eur. J. Clin. Microbiol.*, 2011, **30**, 1067-1073.
- W. Wang, L. Liu, S. Song, L. Tang, H. Kuang and C. Xu, *Sensors-Basel.*, 2015, **15**, 5281-5292.
- J. G. Bruno, *Pathogens*, 2014, **3**, 341-355.
- C.-C. Liu, C.-Y. Yeung, P.-H. Chen, M.-K. Yeh and S.-Y. Hou, *Food. Chem.*, 2013, **141**, 2526-2532.
- A. Singh, H. N. Verma and K. Arora, *Appl. Biochem. Biotech.*, 2015, **175**, 1330-1343.
- J. W. Waswa, C. Debroy and J. Irudayaraj, *J. Food. Process. Eng.*, 2006, **29**, 373-385.
- J. H. Deng, Q. J. Lu, Y. X. Hou, M. L. Liu, H. T. Li, Y. Y. Zhang and S. Z. Yao, *Anal. Chem.*, 2015, **87**, 2195-2203.
- W. Pan, J. Zhao and Q. Chen, *J. Agr. Food. Chem.*, 2015, **63**, 8068-8074.
- Y. P. Chen, Y. L. Xianyu, Y. Wang, X. Q. Zhang, R. T. Cha, J. S. Sun and X. Y. Jiang, *ACS Nano*, 2015, **9**, 3184-3191.
- H. Zhang, Y. Zhang, Y. Lin, T. Liang, Z. Chen, J. Li, Z. Yue, J. Lv, Q. Jiang and C. Yi, *Biosens. Bioelectron.*, 2015, **71**, 186-193.
- A. Ishida, Y. Yamada and T. Kamidate, *Anal. Bioanal. Chem.*, 2008, **392**, 987-994.

18. L. M. Bonanno and L. A. DeLouise, *Adv. Funct. Mater.*, 2010, **20**, 573-578.
19. W. S. Qu, Y. Y. Liu, D. B. Liu, Z. Wang and X. Y. Jiang, *Angew. Chem. Int. Edit.*, 2011, **50**, 3442-3445.
20. Y. Zhou, S. X. Wang, K. Zhang and X. Y. Jiang, *Angew. Chem. Int. Edit.*, 2008, **47**, 7454-7456.
21. Z. Y. Lin, S. Gao, J. Lin, W. L. Lin, S. Y. Qiu, L. H. Guo, B. Qiu and G. N. Chen, *Anal. Methods-Uk.*, 2012, **4**, 612-615.
22. Y. Xianyu, K. Zhu, W. Chen, X. Wang, H. Zhao, J. Sun, Z. Wang and X. Jiang, *Anal. Chem.*, 2013, **85**, 7029-7032.
23. D. B. Liu, J. Yang, H. F. Wang, Z. L. Wang, X. L. Huang, Z. T. Wang, G. Niu, A. R. H. Walker and X. Y. Chen, *Anal. Chem.*, 2014, **86**, 5800-5806.
24. X. Peng, Q. Long, H. Li, Y. Zhang and S. Yao, *Sensor. Actuat B-Chem.*, 2015, **213**, 131-138.
25. Z. Q. Gao, M. D. Xu, L. Hou, G. N. Chen and D. P. Tang, *Anal. Chem.*, 2013, **85**, 6945-6952.
26. X. R. Li, J. Guo, J. Asong, M. A. Wolfert and G. J. Boons, *J. Am. Chem. Soc.*, 2011, **133**, 11147-11153.
27. J. Zhao, Y. Yi, N. Mi, B. Yin, M. Wei, Q. Chen, H. Li, Y. Zhang and S. Yao, *Talanta*, 2013, **116**, 951-957.
28. X. Ji, X. Song, J. Li, Y. Bai, W. Yang and X. Peng, *J. Am. Chem. Soc.*, 2007, **129**, 13939-13948.



Colorimetric and ultrasensitive immunosensor for one-step pathogen detection via the combination of nanoparticles-triggered signal amplification and magnetic separation